Modes of Occurrence and Origin of Minerals in Permian Coals from the Huainan Coalfield, Anhui, China

Yuan Li [1,2,3], **Wenhui Huang** [1,2,3,*], **Bo Jiu** [1,2,3], **Qilong Sun** [1,2,3] and **Qingsong Che** [1,2,3]

[1] School of Energy Resources, China University of Geosciences (Beijing), Beijing 100083, China; liyuan_0710@163.com (Y.L.); jiubo1995@126.com (B.J.); qilong72@gmail.com (Q.S.); cheqs950713@163.com (Q.C.)

[2] Key Laboratory for Marine Reservoir Evolution and Hydrocarbon Abundance Mechanism, China University of Geosciences, Beijing 100083, China

[3] Beijing Key Laboratory of Unconventional National Gas Geology Evaluation and Development Engineering, China University of Geosciences, Beijing 100083, China

* Correspondence: huangwh@cugb.edu.cn

Abstract: Minerals in coal provide useful information for not only paleo-environments of peat accumulation, but also for geological evolution during later diagenesis and/or epigenesis. This paper reports new data on coal quality and the mineralogical and geochemical compositions of 17 unaltered (by intrusion) coal samples collected from the Huainan coalfield, providing new insight into the origins and modes of occurrence of the minerals in coal and their geological evolution. The results showed that the studied coal samples were low rank bituminous coal, with low ash yield (11.92–38.31%, average 24.80%) and high volatile content (25.13–43.43%, average 37.29%). Minerals in the coal mainly included kaolinite and quartz; varying proportions of calcite, siderite, ankerite, and pyrite; and traces of chlorite, zircon, strontianite, apatite, and gorceixite. Typical modes of mineral occurrence could be used to determine the formation stage of minerals. The detrital mineral, occurring as sub-angular to rounded discrete fragments or thin layers intimately admixed with organic matter at particular horizons, was of terrigenous origin, deposited during peat accumulation. Cell infillings, as well as nodule siderites and polycrystalline aggregates of pyrite, precipitated during the syngenetic to early diagenetic stages. Cleat infillings, compressed cell infillings, and fracture infillings precipitated in the epigenetic stage. However, the stage of mineral formation of the pore infilling was difficult to determine. Combined with coal quality, mineralogy, and geochemical analysis, the sedimentary environment of Shanxi Formation was affected by seawater, and Fe-rich hydrothermal fluids filled into the No. 3 coal seam in the epigenetic stage. The sedimentary environment of the No. 8 coal seam had widespread reduction and acid conditions due to basin subsidence, and sulfate-rich hydrothermal fluids may have been formed during the peat deposition stage. In contrast, the peat accumulation environment of the Upper Shihezi Formation was oxidized with a low pH condition. Alkaline fluid then flowed into the No. 13-1 coal seam in the epigenetic stage.

Keywords: minerals in unaltered coal; mode of mineral occurrence; geological significance; Permian coal; Huainan coalfield

---

1. Introduction

Minerals, as inorganic constituents in coal, generally have adverse effects in coal utilization, but they are also considered as potential sources of critical metals [1,2]. From an academic perspective, they can provide a large amount of useful information for understanding coal formation and the geologic history

of coal-bearing strata and individual coal seams because long-term geological evolution from syngenetic to diagenetic and post-diagenetic stages may be recorded within minerals [1,3]. The origins of minerals in coal include river water, flood inputs, airborne dust, volcanic ash, precipitates from underground water, hydrothermal fluid, or others, or may be related to biological activity, especially in modern peat swamps [4,5]. According to the formation stage, minerals can be classified as biogenic, detrital, syngeneic, diagenetic, and epigenetic [5,6]. Syngenetic minerals formed during or shortly after peat accumulation; epigenetic minerals precipitated from solutions that percolated through the coal after the coal's compaction, lithification, and rank advance [5–7]. Minerals may have been affected and altered by interaction with fluids that permeated through the coal seam or the heat of the igneous intrusions [8,9].

Previous studies showed that some minerals are useful indicators of geological evolution. Liu discussed the influence of sedimentary environments on the content of minerals in coal based on 18 coal samples in China [10]. Kong et al. reported that Jurassic coal formed in a terrigenous sedimentary environment because no pyrite was identified by XRD in Beipiao coal, Liaoning, China [11]. Spiro et al. revealed that the $^{87}Sr/^{86}Sr$ values of the gypsum in coal can be used as a chronometer to determinate a temporal framework for geological processes during the Miocene age [12]. Some typical minerals and their occurrence may indicate an effect of igneous intrusion. The carbonate minerals and pyrite occurring as epigenetic cleat- and fracture-fillings were probably derived from igneous fluids [13,14]. NH_4-illite may have been formed by an interaction of kaolinite with nitrogen released from coal organic matter caused by the igneous intrusion [15]. Gibbsite subjected to dehydration by the heat of the igneous intrusion may have been altered to diaspore [16]. In the northern Huainan coalfield, including the Dingji, Zhuji, and Pan3 mines, igneous intrusion events were reported and the effects on coal quality, chemical and mineralogical compositions, and coalbed methane characteristics were investigated [17–19]. Miao et al. determined the magmatic intrusive age and discussed its geological significance in the Pan3 mine [20].

However, few have investigated the occurrence modes and origins of minerals in coal in the non-igneous intrusion area in the Huainan coalfield. This paper reports the mineralogical and geochemistry characteristics of Permian coal in the Huainan coalfield; the main research was conducted in the P1 mine, involving five coal seams of Nos. 1, 3, 8, 11-2, and 13-1. Our aims were (1) to investigate the relationship between the modes of mineral occurrence and the processes of mineral formation, and (2) to understand the geological evolution of Permian coal-bearing seams in the Huainan coalfield.

2. Geological Setting

The Huainan coalfield is located in the southeastern North China Plate. The coalfield covers an area of more than 2000 km^2, 75 km in length and 25 km in width (Figure 1). The coal-bearing strata in the Huainan coalfield mainly contain the Late Carboniferous Taiyuan Formation, the Early Permian Shanxi Formation, the Middle Permian Lower Shihezi Formation, and the Late Permian Upper Shihezi Formation. The coal seams from the Taiyuan Formation are not economically minable due to their thin thickness and discontinuity. However, the Permian strata generally contain 40 layers of coal and in a few cases, up to 56 layers. The total thickness of the coal seams in the Permian strata is 30–40 m, and the minable thickness of the coal seams is 23–26 m. The No. 13-1 and No. 11-2 coal seams in the Upper Shihezi Formation, No. 8 seam in the Lower Shihezi Formation, and Nos. 1 and 3 seams in the Shanxi Formation were sampled in this study.
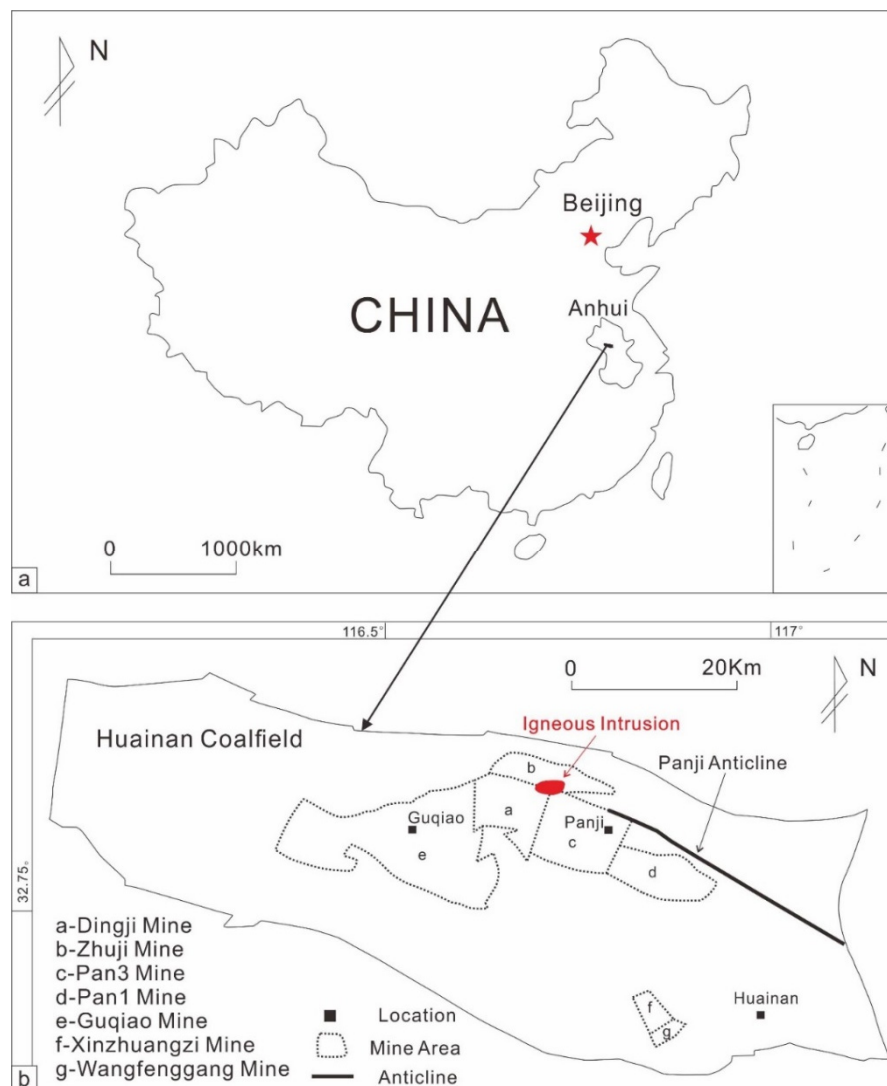
Figure 1. (**a**) Location and (**b**) details in Huainan coalfield (modified from [21–23]).

From the Early Permian to the Middle Permian, the Huainan coalfield underwent repeated marine transgression and regression in which the marine regression toward the south was dominant [24,25]. Lan et al. [26] first described the evolution of the Permian strata, from the Shanxi Formation deposited in a tidal-flat delta influenced by brackish water, to the Lower Shihezi Formation deposited in a lower delta plain occasionally influenced by seawater incursion, to the Upper Shihezi Formation deposited in an upper delta plain. According to the boron content in the rock, Sun et al. [27] concluded that all the Permian strata were affected by seawater and fresh water alternately, whereas Chen et al. [28] argued that the Shanxi Formation was influenced by persistent seawater. Zhao et al. [29] contrasted the distribution patterns of rare earth elements (REE) in each formation of the Permian strata. The results also suggested that the depositional environment of the Shanxi Formation was different from that of the Upper Shihezi and Lower Shihezi Formations.

During the early Cretaceous, multiple tectonic activities occurred with different intensities of magmatic activity in the Huainan coalfield, and the Mesozoic Yanshanian magmatic activity was the most intense [19]. From No. 17-1 to No. 1, coalbeds were influenced by the igneous intrusion to various extents, although the lower part was more seriously damaged than the upper [20,30]. The intrusive rocks were mainly distributed in the south wing of Panji anticline, including aplite, syenite porphyry, and lamprophyre. The coal quality and rank, to some extent, were changed by the activity of igneous intrusions [31]. However, igneous intrusion has only been reported in the northern section of the

Huainan coalfield, including the Dingji, Zhuji, and Pan3 mines [22,27,30]. The stratigraphic and lithologic characteristics of Permian strata in the Pan1 mine are depicted in Figure 2.
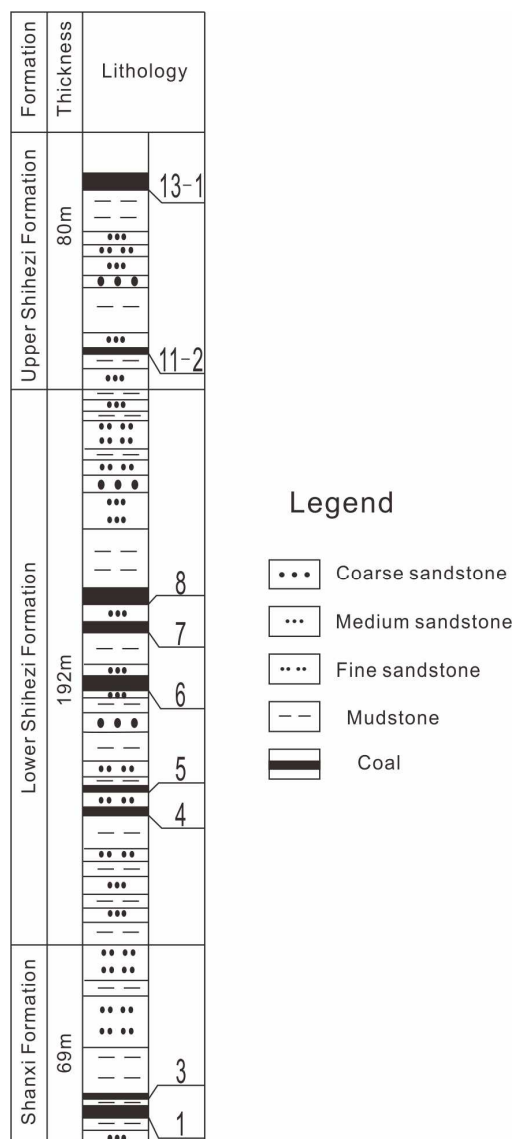

Figure 2. Generalized stratigraphic column of the Permian coal in the Pan1 mine of the Huainan coalfield.

3. Materials and Methods

A total of 17 coal samples were collected from Permian coalbeds in different boreholes at four coal mines, of which 14 coal samples were obtained from four boreholes in the Pan1 mine (P1) (Table 1), and the remaining three were from the Guqiao mine (GQ, No. S10), Wangfenggang mine (WFG, No. S6), and Xinzizhuang mine (XZZ, No. S11) in the Huainan coalfield (Figure 1). All samples were immediately stored in plastic bags to prevent contamination and oxidation.

Coal proximate analyses including ash yield, moisture, and volatile matter were determined in accordance with ASTM Standards D3174-12 (2018), D3173/D3173M-17 (2017), and D3175-18 (2018) [32–34], respectively. Total sulfur was measured following ASTM Standard D4239-18e1 (2018) [35].

Polished epoxy-bound particulate pellets were prepared to observe the optical characterizations of minerals under the reflected lights of a Leitz Laborlux 12POL optical microscope (Leica Microsystems, Wetzlar, Germany).

A scanning electron microscope (JSM-6700F, JEOL, Tokyo, Japan) in conjunction with an energy-dispersive X-ray spectrometer (INCA, Oxford Instruments, High Wycombe, UK) were used to identify the minerals and some elements in the coal. The operating parameters were set to 20 kV acceleration voltage, high vacuum mode.

The samples used for X-ray fluorescence spectrometry (XRF) and X-ray diffraction (XRD) analysis were crushed and ground to less than 200 mesh. A Rigaka D/Max-RC powder diffractometer (Rigaku Corporation, Tokyo, Japan) with Cu-Kα1 radiation was used to determine the mineral compositions of the raw coal samples. The diffractograms were obtained at 40 kV and 80 mA. The XRD pattern was recorded over a 2θ interval of 10–60° and a step size of 0.01°. Semiquantitative mineralogical analysis was performed using the matrix-flushing method devised by Chung [36], also known as the K value method. The K value is a constant determined by each crystalline phase and the internal standard. The powder coal samples under study were spiked with the internal standard (fluorite) using the XRD intensity ratio between a crystalline phase and an internal standard and constant K to obtain the proportions of each crystalline phase of the sample.

Powder coal samples were ashed in a muffle furnace at 815 °C. The concentrations of the major element oxides of coal ash were determined by XRF (Thermo ADVANT XP+, Thermo Fisher, Waltham, MA, USA), including SiO_2, Al_2O_3, CaO, K_2O, Na_2O, Fe_2O_3, SO_3, MgO, and TiO_2. The borate fusion technique was used. Each ash sample (1 g) was mixed with a mixed flux (10 g, 50% $Li_2B_4O_7$ + 50% $LiBO_2$) in a 95% Pt/5% Au crucible. The crucible was heated in a Globar furnace. These two points were followed to obtain more accurate and precise sulfur content: (1) heat for 10 min at 700 °C to convert the sulfur completely to SO_3; (2) raise the temperature until the flux melts, but keep the heating temperature below 1000 °C to prevent sulfur volatilization. The results were normalized to indicate the concentrations of the major element oxides in the inorganic fraction of each coal sample.

Table 1. Proximate analyses (%) and total sulfur (%) of the coal samples from the Huainan coalfield.

Coal Mine	Borehole	Coal Seam No.	Sample No.	M_{ad}	A_d	V_{daf}	$S_{t,d}$
P1	B1-9	13-1	S1	1.30	32.39	41.33	0.20
P1	B1-1	13-1	S2	1.48	29.60	43.41	0.13
P1	B2-3	13-1	S4	0.72	29.76	36.29	0.13
WFG *	-	13-1	-	0.75	23.05	25.13	nd
P1	B1-9	11-2	S7	1.02	21.96	38.02	0.21
P1	B1-2	11-2	S8	1.02	17.23	37.53	0.26
P1	B2-3	11-2	S9	0.66	20.83	34.17	0.41
P1	B1-9	8	S12	1.08	38.31	37.34	0.31
P1	B1-1	8	S13	1.06	35.89	41.40	0.43
P1	B1-2	8	S14	1.14	31.47	38.88	0.29
P1	B2-3	8	S15	0.78	25.91	35.02	0.69
GQ **	-	8	-	nd	nd	nd	1.20
XZZ **	-	8	-	nd	nd	nd	0.69
P1	B1-9	3	S16	1.02	16.86	36.23	0.42
P1	B1-2	3	S17	0.89	11.92	36.66	0.51
P1	B1-9	1	S18	0.96	17.56	36.25	0.63
P1	B1-2	1	S19	1.10	19.21	35.66	1.51

Note: M, moisture; A, ash yield; V, volatile matter; St, total sulfur; ad, air-dry basis; d, dry basis; daf, dry and ash-free basis; nd, no data; * From Ao [37]; ** From Jiang et al. [38].

4. Results

4.1. Coal Quality Parameters

The data of proximate analysis and forms of sulfur for each studied coal sample are listed in Table 1. The ash yield of the coal samples varied between 11.92% and 38.31% (24.80% on average). Most of them were medium to high ash coal according to Chinese National Standards (GB/T 15224.1-2018 [39], 10.01–20.00% for low ash coal, 20.01–30.00% for medium ash coal, and 30.01–40.00% for high ash coal).

The volatile matter ranged from 25.13% to 43.41% (36.89% on average), corresponding to a high volatile A bituminous to medium volatile bituminous coal rank (ASTM D388-15 [40]). The total sulfur content ranged from 0.13% to 1.51% (average 0.50%) and mostly belonged to ultra-low sulfur coal according to the Chinese standard classification for sulfur (GB/T15224.2-2010 [41]). The moisture contents of all samples ranged from 0.66% to 1.48%, with an average of 1.00%.

4.2. Major Elements in the Coal

The percentages of major element oxides in Permian coals from the Huainan coalfield are dominated by SiO_2 and Al_2O_3, and the details are provided in Table 2.

Table 2. Concentration of major element oxides (%) of the coal samples from the Huainan coalfield.

Coal Mine	Borehole	Coal Seam No.	Sample No.	SiO_2	TiO_2	Al_2O_3	Fe_2O_3	MgO	CaO	Na_2O	K_2O	SO_3
P1	B1-9	13-1	S1	53.90	1.21	33.51	3.73	1.11	3.94	0.66	1.01	0.93
P1	B1-1	13-1	S2	56.87	0.73	29.57	4.95	1.30	5.16	0.29	0.42	0.70
P1	B2-3	13-1	S4	56.47	1.26	30.58	4.03	1.10	4.17	0.46	1.07	0.87
P1	B1-9	11-2	S7	56.39	0.97	31.84	4.28	1.21	2.72	0.66	1.31	0.64
P1	B1-2	11-2	S8	52.83	1.23	34.38	5.33	1.06	2.50	0.41	1.42	0.83
P1	B2-3	11-2	S9	57.68	1.28	31.76	4.81	0.46	1.11	0.46	1.44	1.00
GQ	B3-1	8	S10	53.69	0.96	32.51	5.53	1.05	2.63	0.41	0.61	2.62
XZZ	B3-2	8	S11	57.38	1.16	30.84	5.37	0.56	1.24	0.68	1.14	1.65
P1	B1-9	8	S12	60.32	1.05	27.69	4.58	1.03	2.51	0.48	1.11	1.23
P1	B1-1	8	S13	56.54	1.25	31.72	4.47	1.03	2.63	0.41	0.71	1.25
P1	B1-2	8	S14	58.73	1.08	30.48	3.75	0.99	2.24	0.51	1.02	1.19
P1	B2-3	8	S15	58.51	1.21	30.27	5.09	0.51	1.18	0.53	1.37	1.32
P1	B1-9	3	S16	49.22	1.00	27.33	4.52	2.25	10.99	0.87	1.01	2.81
P1	B1-2	3	S17	55.56	1.07	24.72	3.88	1.88	7.15	0.41	1.27	4.06
P1	B1-9	1	S18	43.49	0.98	29.65	5.28	2.32	11.58	0.51	0.89	5.30
P1	B1-2	1	S19	45.69	1.52	28.86	9.53	1.67	6.09	0.41	1.57	4.65

In this study, most of Al and Si consist of clay minerals (kaolinite and chlorite), and some Si occurs in quartz. Fe can be found in chlorite, carbonate minerals (siderite, ankerite), pyrite, and other common iron-rich minerals. The percentages of CaO, MgO, and SO_3 in the Shanxi Formation were significantly higher than in the Lower and Upper Shihezi Formation. The element assembles in Nos. 1 and 3 coal seams were similar, having relatively high contents of Ca and S. The S was slightly enriched in the Lower Shihezi Formation No. 8 coal seam. For the Upper Shihezi Formation, the No. 13-1 coal seam was similar to the No. 11-2 coal seam except for the obviously elevated C content. Although the specific reasons for the element content changes should be analyzed in combination with the mineral composition and the mode of mineral occurrence, a relationship exists between these changes and the environment of the peat accumulation stage or later than that. The cause of enrichment of every element is discussed in Section 5.2.

4.3. Mineral Compositions in the Coal

The contents of each mineral identified by the XRD analysis of raw coal samples are provided in Table 3. The mineral assemblage in the coal samples mainly consisted of kaolinite, and varying proportions of quartz, calcite, and pyrite. Kaolinite is the most common clay mineral in high- to medium-volatile bituminous coal [42], and is also considered a terrestrial source mineral far from the marine depositional environment [43]. Pyrite was enriched in the No. 8 coal seam from different mine areas of the Huainan coalfield, while calcite was less. The slightly high content of S in the No. 8 coal seam occurred in response to the high pyrite percentage. The minerals in the No. 11-2 coal seam were mostly composed of kaolinite and quartz.

Table 3. Mineralogical composition of raw coal samples (%) determined by X-ray diffraction.

Coal Mine	Borehole	Coal Seam No.	Sample No.	Clay	Quartz	Calcite	Pyrite
P1	B1-1	13-1	S2	84.9	5.2	9.9	bdl
WFG	B3-3	13-1	S6	82.6	5.6	11.2	0.7
P1	B2-3	11-2	S9	88.9	10.9	0.2	bdl
GQ *	-	8	-	67.6	8.4	1.6	22.5
XZZ *	-	8	-	74.1	5.6	1.9	18.5
P1	B1-2	8	S14	77.6	5.2	3.4	13.8
P1	B1-9	3	S16	83.4	8.3	8.4	bdl
P1	B1-2	3	S17	88.2	11.4	0.4	bdl
P1	B1-9	1	S18	77.9	10.7	11.4	bdl
P1	B1-2	1	S19	77.6	15.2	7.1	bdl

Note: bdl, below detected limit; * From Jiang et al. [38].

4.4. Modes of Mineral Occurrence

The modes of mineral occurrence in these coals were mainly examined by SEM-EDS and an optical microscope with reflected light (Figures 3–7).

4.4.1. Quartz

Some quartzes occur as sub-angular to sub-rounded grains surrounded by dispersedly compacted layers of clay matrix (Figure 3a). The grain size of these quartzes was between 5 and 10 μm, which is silt sized. Some quartzes occurred as pore infillings in intercrystalline pores and dissolved pores (Figure 3b).
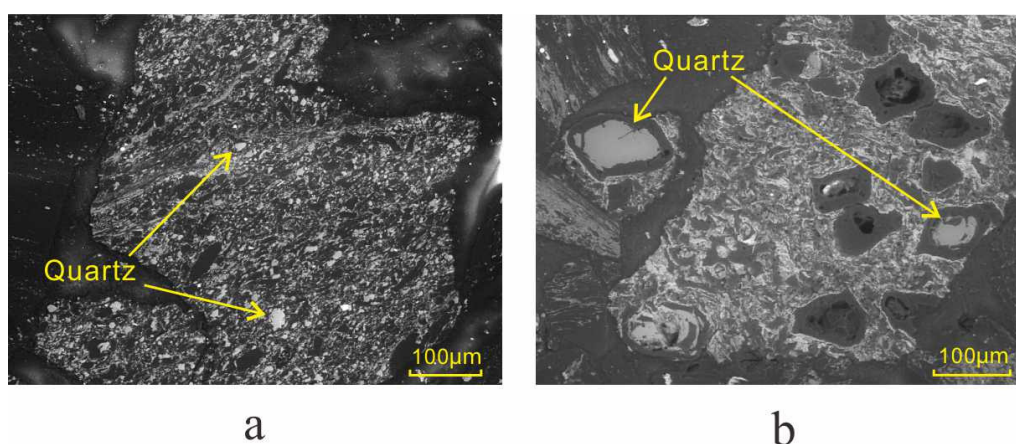

Figure 3. SEM back-scattered electron images of quartz in the Huainan coalfield. (**a**) Quartz occurring as sub-rounded particles embedded in kaolinite matrix, S15, Pan1 (P1) mine, No. 8 coal seam; (**b**) quartz occurring as pore space infillings in a dissolved pore, S10, Guqiao (GQ) mine, No. 8 coal seam.

4.4.2. Clay Minerals

Kaolinite was the dominant clay mineral in the studied coal samples. There were two kinds of occurrences of kaolinite. The first type of kaolinite occurred as a matrix (Figure 4a), and, in some cases, was intimately admixed with organic matter and distributed along bedding (Figure 4b). The second type was fine grained kaolinite, occurring as infillings in cell lumens (Figure 4c) or fractures (Figure 4d). In addition, minor amounts of chlorite were observed under the SEM-EDS, occurring as compressed cell infillings (Figure 4e,f) in the No. 3 coal seam from the P1 mine.
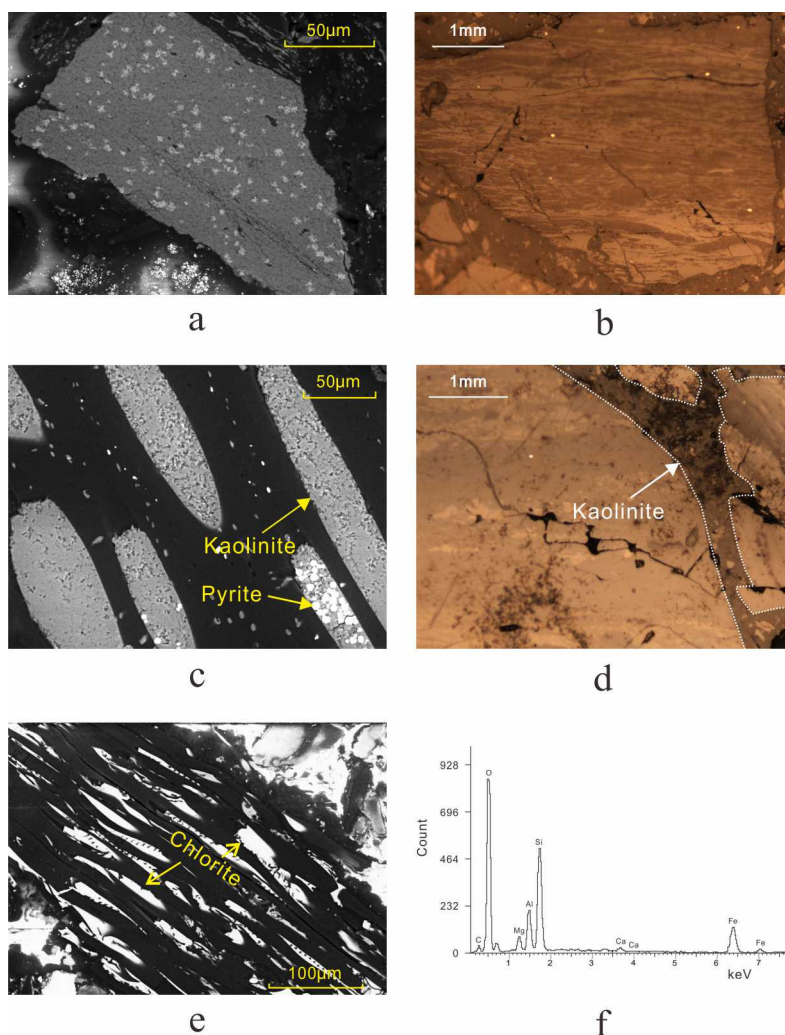
Figure 4. Clay minerals in the coal of Huainan coalfield. (**a**) Kaolinite occurring as a matrix under the SEM, S11, Xinzizhuang (XZZ) mine, No. 8 coal seam; (**b**) kaolinite intimately admixed with maceral under an optical microscope, reflected light, S9, P1 mine, No. 11-2 coal seam, 200×; (**c**) kaolinite occurring as cell infillings intergrown with pyrite under a SEM, S10, GQ mine, No. 8 coal seam; (**d**) kaolinite occurring as fracture infillings under an optical microscope, reflected light, S9, P1 mine, No. 11-2 coal seam, 200×; (**e**) chlorite occurring as compressed cell infillings under a SEM, S16, P1 mine, No.3 coal seam; (**f**) X-ray EDS spectrum of chlorite in panel (**e**).

4.4.3. Carbonate Minerals

Carbonate minerals, including calcite, ankerite, and siderite, were identified by SEM-EDS. In most cases, carbonate minerals were of authigenic origin as pore infillings (Figure 5a), or cleat and fracture infillings. In a few cases, calcite coexisted with quartz or ankerite (Figure 5b,c). Ankerite also occurred as pore fillings (Figure 5d). Strontianite was only present as cell lumen infillings in small proportions (Figure 5e,f). Siderite was found as ellipsoidal nodules (Figure 5g) that bend the surrounding clay minerals and organic matter bands. Siderite was also found in the form of compressed cell infillings (Figure 5h,i) in coals.
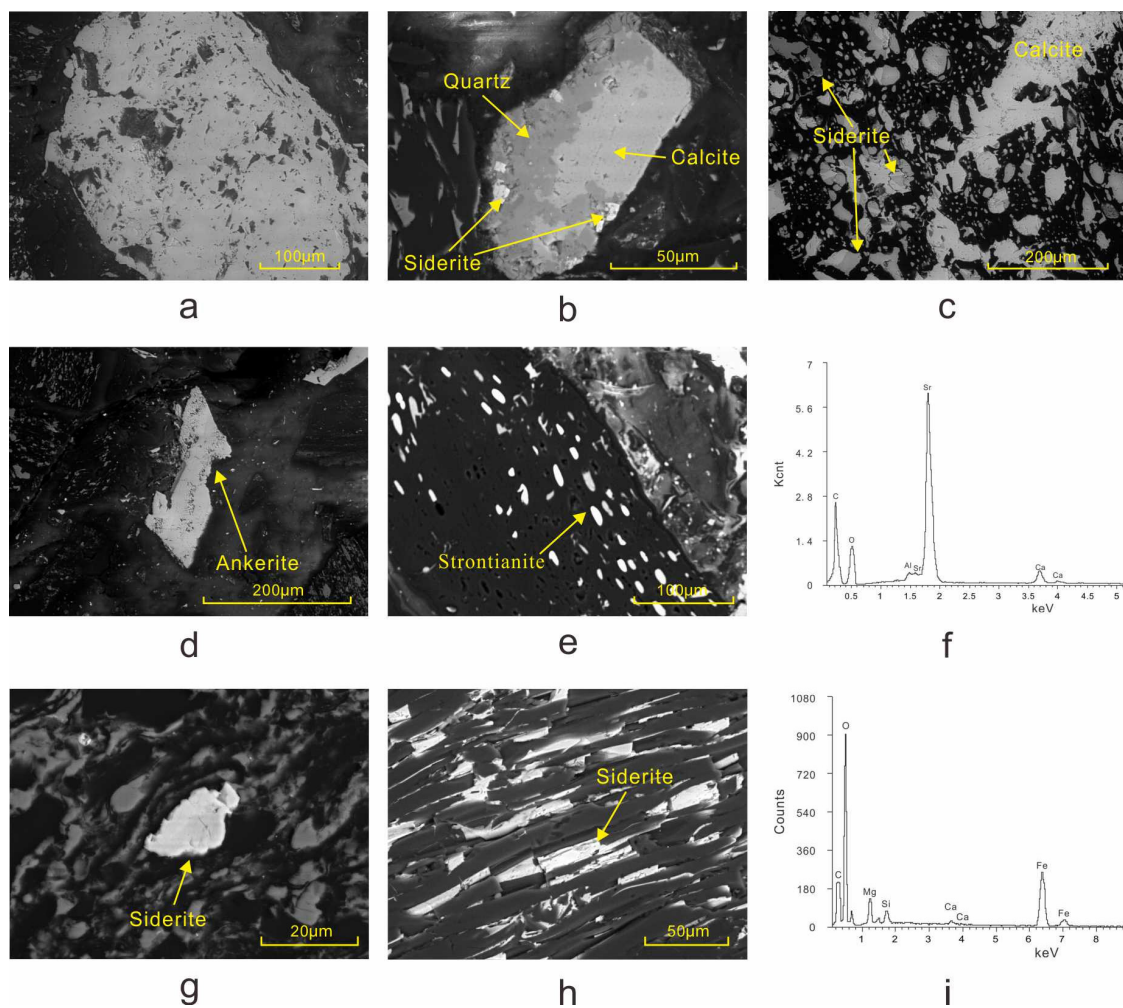
Figure 5. SEM back-scattered electron images of carbonate minerals in the coals of Huainan coalfield. (**a**) Authigenic calcite occurring as pore infillings, S2, P1 mine, No. 13-1 coal seam; (**b**) preexisting quartz replaced partly by calcite, S2, P1 mine, No. 13-1 coal seam; (**c**) intergrown ankerite and calcite, S6, Wangfenggang (WFG) mine, No. 13-1 coal seam; (**d**) ankerite occurring as pore infillings, S2, P1 mine, No. 13-1 coal seam; (**e**) strontianite occurring as pore infillings, S18, P1 mine, No. 1 coal seam; (**f**) X-ray EDS spectrum of strontianite in panel (**e**); (**g**) siderite as ellipsoidal nodules surrounded by deformed maceral and clay layers, S2, P1 mine, No. 13-1 coal seam; (**h**) siderite occurring as compressed cell infillings, S6, WFG mine, No. 13-1 coal seam; and (**i**) X-ray EDS spectrum of siderite in panel (**h**).

4.4.4. Pyrite

Pyrite is the most common sulfide mineral in many coal seams [5,6]. The pyrite was identified by SEM in two forms of polycrystalline aggregates. The first one occurred in a framboidal form generally 10 μm or so in size and spherical in shape. Framboids were composed of small euhedral crystals, with the crystals aggregated into an overall spherical form (Figure 6a). The euhedral pyrite crystals of framboids were generally 1 μm or so in size and octahedral in shape (Figure 6b). The second one occurred as massive aggregates that consisted of multiple pyritohedral crystals (Figure 6c,d). This type of pyrite was larger than the first, about 100 μm in size.
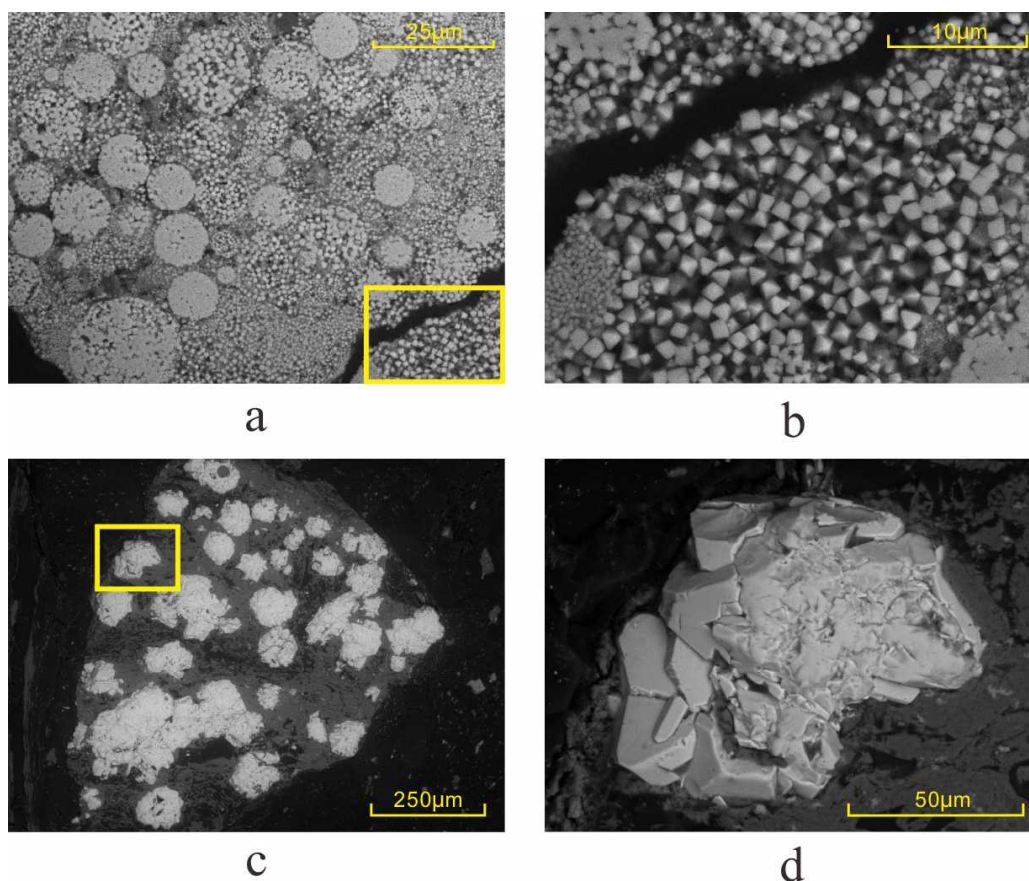
Figure 6. SEM back-scattered electron images of pyrite in the coals of Huainan coalfield. (**a**) Pyrite aggregates occurring as framboids, S10, GQ mine, No. 8 coal seam; (**b**) euhedral pyrite crystals surrounded framboidal pyrite, an enlarged image of the yellow rectangle in (**a**); (**c**) pyrite aggregates occurring as a massive form, S11, XZZ mine, No. 8 coal seam; (**d**) a pyritohedral pyrite crystal, an enlarged image of the yellow rectangle in (**c**).

4.4.5. Other Minerals

Well-rounded trace proportions of zircons were observed by SEM, mostly ranging from 5 to 10 μm, distributed in organic matter and the kaolinite matrix (Figure 7a,b). The occurrence of apatite found in the S11 coal sample was scattered over the kaolinite (Figure 7c,d). The mineral occurring as cell infillings in the S6 coal sample was gorceixite according to X-ray EDS spectra (Figure 7e,f), which is a kind of Ca- and Ba-rich aluminophosphate mineral.
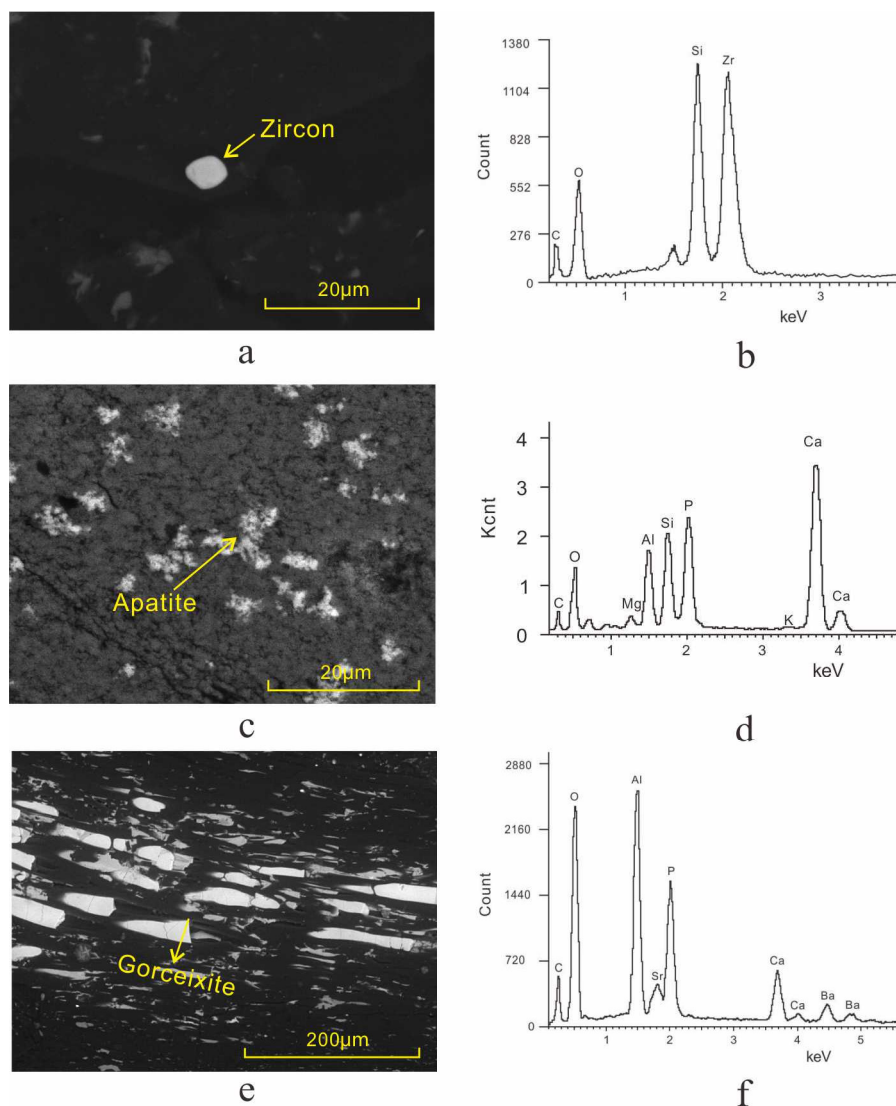
Figure 7. SEM back-scattered electron images and X-ray EDS spectrograms of minerals in the coals of Huainan coalfield. (**a**) Zircon occurring as a sub-round grain, S15, P1 mine, No. 8 coal seam; (**b**) X-ray EDS spectrum of zircon in (**a**); (**c**) apatite scattered over the kaolinite, S11, XZZ mine, No. 8 coal seam; (**d**) X-ray EDS spectrum of apatite in (**c**); (**e**) gorceixite occurring as cell infillings, S6, WFG mine, No. 13-1 coal seam; and (**f**) X-ray EDS spectrum of gorceixite in (**e**).

5. Discussion

5.1. Origin of Minerals in the Coal Samples

5.1.1. Detrital Input

Detrital mineral material, including some of the mineral particles, was introduced into the peat accumulation environments by river water and flood inputs, airborne dust, and other epiclastic processes. These detrital minerals generally occur as sub-angular to rounded discrete fragments or thin layers intimately admixed with the organic matter at particular horizons [6,44].

The silt-sized quartz (Figure 3a) in the No. 8 coal seam of P1 mine was most likely of detrital origin, introduced into the peat swamp by water flow from the swamp margin, in accordance with the characteristics of detrital quartz from the results reported by Ward [45]. Kaolinite is the dominant mineral in bituminous coal, decreasing and even disappearing the anthracite [46]. The kaolinite

admixed with organic materials distributed along bedding planes (Figure 5b) in the No. 11-2 coal seam of the P1 mine formed from the same detrital origin.

Dai et al. found that the detrital zircon in the No. 6 coal seam of the Junger coalfield was derived from the Benxi Formation bauxite [47]. The weathered crust of Benxi Formation in Northern China contains heavy minerals, such as zircon, rutile, and galena [47]. It is likely that the well-rounded zircon in the No. 8 coal seam of the P1 mine (Figure 7a) was a detrital material of terrigenous origin transported into the peat mire from bauxite by the fluvial system.

5.1.2. Syngenetic and Early Diagenetic Precipitation

In the syn-depositional and early diagenetic stages, the peat layer is not compressed or slightly compressed, so cell infilling is a typical mode of occurrence of syngenetic minerals. For example, the kaolinite in the form of a flat lens (Figure 6c) in the No. 8 coal seam of the GQ mine, the strontianite in the No. 1 coal seam of the P1 mine (Figure 5e), and the gorceixite in the No. 13-1 coal seam of the WFG mine (Figure 7e) were all formed by the precipitation of fluids during the syn-depositional to early diagenetic stages. The precipitation of the gorceixite requires low pH (pH < 3) and oxidizing conditions [48]. Al may have been derived from the bauxite on the weathered crust surface of the Benxi Formation in the sediment-source region [9]. Oxidation conditions facilitate the leaching of phosphorus from organic matter during plant decay [48]. Dissolved Al, Si, Ba, Ca, and P transferred with swamp water to someplace in the peat deposit in which pH conditions were suitable for precipitation. Syngenetic kaolinite precipitates from Al- and Si-rich fluids in acidic conditions. The strontianite precipitates from a Sr-rich fluid derived from seawater. Apatite and gorceixite are formed in a similar precipitation process. The difference is that aluminum is available when gorceixite is formed, whereas there is no Al when apatite is formed. The apatite was scattered over the kaolinite matrix in the No. 8 coal seam of the XZZ mine (Figures 4a and 7c), indicating that apatite was deposited in the intercrystalline pores of kaolinite after kaolinite formation.

Nodule siderite and polycrystalline aggregates of pyrite are also typical syngenetic minerals. Nodule siderite is commonly formed in a reducing and sulfur-poor environment that allows ferrous ions to combine with carbonate to form siderite. The nodule siderite in the No. 13-1 coal seam (Figure 5g) was clearly formed in the syngenetic stages because the clay minerals and organic matter bands around it are bent. In addition to a reducing condition, the most favorable pH for siderite formation is 7–7.8. If Mg^{2+} and Ca^{2+} are available, syngenetic ankerite forms in reducing and more alkaline conditions (pH > 7.8) [8]. The framboidal pyrite forming processes have been discussed broadly. It can be the result of pyritization of bacteria [49] or abiotic transformations within the Fe-S system [50,51]. Kostova et al. distinguished the difference of textures and morphology between bacterial and inorganic framboidal pyrite. Bacterial framboidal pyrite does not contain euhedral pyrite, while the microcrystals in inorganic framboidal pyrite are octahedral, pentagonal dodecahedral, and cubic [52]. The pyrite in No. 8 coal seam of study area was clearly of inorganic origin. The Lower Shihezi formation where the No. 8 coal seam is located was developed in a transitional zone environment of lower and upper deltaic plains without or with weak seawater influence [27,53–55]. Considering its depositional environment and the modes of occurrence, the pyrite in the No. 8 coal seam was probably derived from hydrothermal fluids. Butler and Rickard experimentally determined that the formation of framboidal pyrite in the hydrothermal system is reasonable [56]. The mechanism of the reaction was proposed by Rickard and Luther [57]. Although coexisting pyrite and siderite were not common, the presence indicates the pH changed from slightly acidic through neutral to slightly alkaline [8], and syngenetic pyrite formed prior to siderite.

5.1.3. Epigenetic Precipitation

In the diagenetic stage, peat layers gradually lithify into coal seams. Following compaction and rank advance, cell cavities that unfilled became compressed and cleats appeared. Therefore, cleat infillings and compressed cell infillings probably indicate epigenetic deposition, such as the chlorite in

the No. 3 coal seam of the P1 mine (Figure 4e) and siderite in the No. 13-1 coal seam of the WFG mine (Figure 5h). Fracture infilling is another typical mode of occurrence of epigenetic minerals, like the kaolinite in the No. 11-2 coal seam of the P1 mine (Figure 4d).

Except for nodule siderite, most carbonate minerals formed in the epigenetic stage. Carbonate minerals dissolve in acid conditions, so the precipitation of the calcite and ankerite (Figure 5a,d) in the No. 13-1 coal seam of the P1 mine and the ankerite occurring as fracture infillings in the No. 13-1 coal seam of the WFG mine (Figure 5c) indicate an alkaline fluid in the pore space.

In many studies, chlorite is regarded as one of the representative minerals in anthracite coal [7,58]. However, in a few cases, chlorite is also present in low-rank coal, which seems related to low-temperature hydrothermal fluids [59,60]. In the study area, chlorite also occurs in medium-high to high volatile matter bituminous coals. The mode of occurrence of chlorite in the No. 3 coal seam of the P1 mine suggests that it formed from Fe-rich hydrothermal fluids filling in the cleats.

Epigenetic minerals can also be precipitated or changed in relation to diagenetic activity (e.g., dissolution and metasomatism), tectonism, and magmatic activity. For example, the quartz in the No. 8 coal seam of the GQ mine (Figure 3b) precipitated in the dissolution pore. Preexisting quartz may have been partly displaced by calcite in the No. 13-1 coal seam of P1 mine (Figure 5b) due to the alkaline solutions permeated into the coal seam and the fracture-filling minerals formed by migration fluids flowing into fractures after epigenetic tectonic activities.

Notably, pore filling is a special mode of mineral occurrence that cannot be used to determine the stage of mineral formation. Pores are formed from the peatification stage through the coalification stage to the epigenetic stage, so pore filling can occur in every stage of peat accumulation to epigenesis.

5.2. Implication for Geological Evolution

The ash yield of coal seams in the Shanxi Formation was significantly lower than in the Upper and Lower Shihezi Formations (Figure 8) due to their coal-forming environment. Coals in the Shanxi Formation were deposited in a subaqueous deltaic plain environment with marine regressions; coals in the Lower Shihezi Formation were developed in a transitional zone of lower and upper deltaic plains; coals in the Upper Shihezi Formation were formed in a fluvial channel system on the deltaic plain [26,28,54,55,61]. The influence of marine water and less input of terrigenous clastics in the Shanxi Formation collectively led to its lowest ash yields in the three formations. Although the Lower and Upper Shihezi Formations both developed in a fluvial affected deltaic plain environment, the ash yield in the Lower Shihezi Formation was higher than in the Upper Shihezi Formation (Figure 8). This trend also appears in the Dingji mine [53], mainly due to the relatively high accommodation/peat accumulation ratio or high groundwater table of the peat mire favoring minerals accumulation [62] during the Lower Shihezi Formation period, when the basin underwent an accelerating basin subsidence [53]. The accelerating basin subsidence resulted in a rising groundwater table and increasing detrital input [53], such as detrital zircon and quartz. The reasons for the high ash yield of the No. 13-1 coal seam are related to terrigenous detritus input and epigenetic hydrothermal minerals.

Although the volatile content in the WFG mine was low, it was still within the volatile content range of unaltered (by intrusion) coal. Ao [37] found that the volatile content of WFG coal was generally less than 30%; the correlation of volatile matter with depth is shown in Figure 9a. The author contended that the WFG mine plutonic metamorphism and dynamic metamorphism may be the main reasons for the low volatile content rather than contact metamorphism. Previous studies showed that coals altered by intrusion from most basins are characterized by increasing ash yield and decreasing volatile matter near the intrusion [13,14,63]. However, all samples in this study displayed a positive correlation between ash yield and volatiles; the range of volatiles was higher than that of the altered coals (Figure 9b). Therefore, we confirmed that the samples in our study area were unaltered coals.

For the Shanxi Formation, significantly high percentages of CaO, MgO, and SO_3 suggest that it developed in a subaqueous deltaic plain environment influenced by seawater. The origin of strontium in strontianite in the No. 1 coal seam is also likely from seawater.
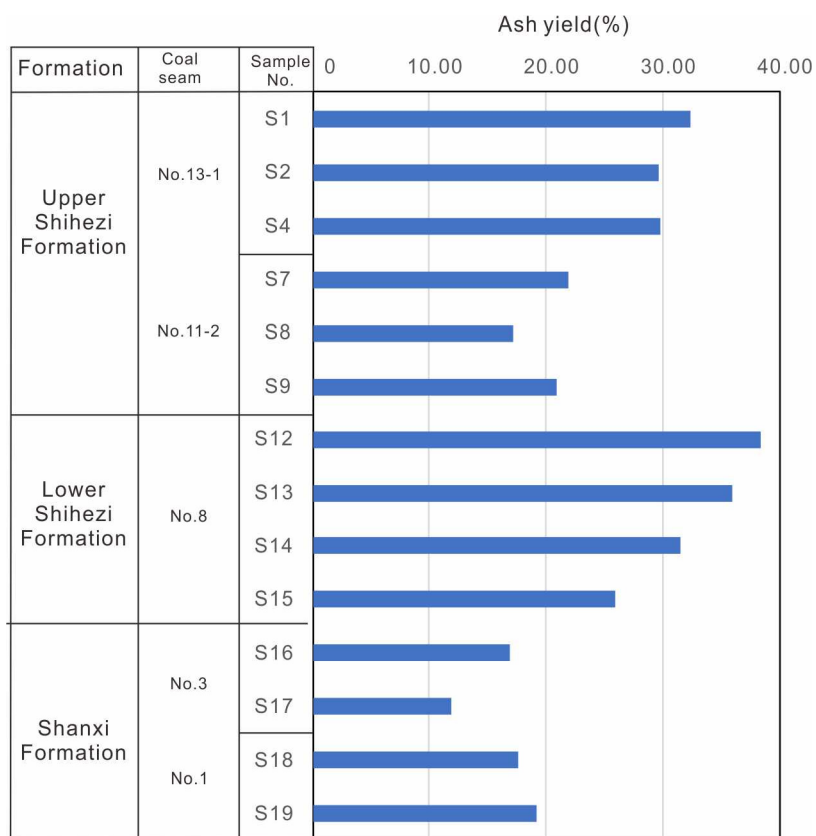
Figure 8. Variation of ash yield from studied coal samples of the three formations.

For the Lower Shihezi Formation, kaolinite, pyrite, and apatite were the main minerals in the No. 8 coal seam. They were all stable under acidic conditions formed in syngeneic stage, which indicates an acidic peat accumulation environment. The modes of occurrence of pyrite suggest an inorganic origin during early diagenetic stage, which indicates that sulfate-rich hydrothermal fluids may have existed during peat deposition stage. The formation of pyrite requires a reducing environment for bacterial reduction of sulfate ions [64,65], followed by H_2S reacting with the dissolved iron to form pyrite. Syngenetic pyrite can derive from not only marine influenced environments but also freshwater dominated environments [5,65,66]. Therefore, it is not a useful mineral for distinguishing sedimentary environments, but a typical mineral formed in reductive environments.

In contrast, the Upper Shihezi Formation formed in an oxidation and acidic peat accumulation environment. The high proportion of kaolinite and gorceixite-forming material may have been derived from the exposed bauxite of the Benxi Formation in the sediment source region. The peat sedimentary environment subjected to oxidation was conducive to the formation of low pH conditions (e.g., pH < 3), under which Al and other ions could be leached from detrital materials. The No. 13-1 coal seam had a high ash yield, which was attributed to the carbonate minerals in coal, unlike that of the No. 11-2 coal seam (S6–S9). The epigenetic carbonate minerals in the No. 13-1 coal seam suggested that alkaline solutions permeated into the coal seam during the late diagenetic to epigenetic stage. However, these epigenetic minerals may have derived from either a hydrothermal fluid that carried CO_2 or alkaline groundwater. In addition, the existence of fracture infills in the No. 11-2 coal seam indicates that epigenetic tectonic movements occurred after diagenesis.
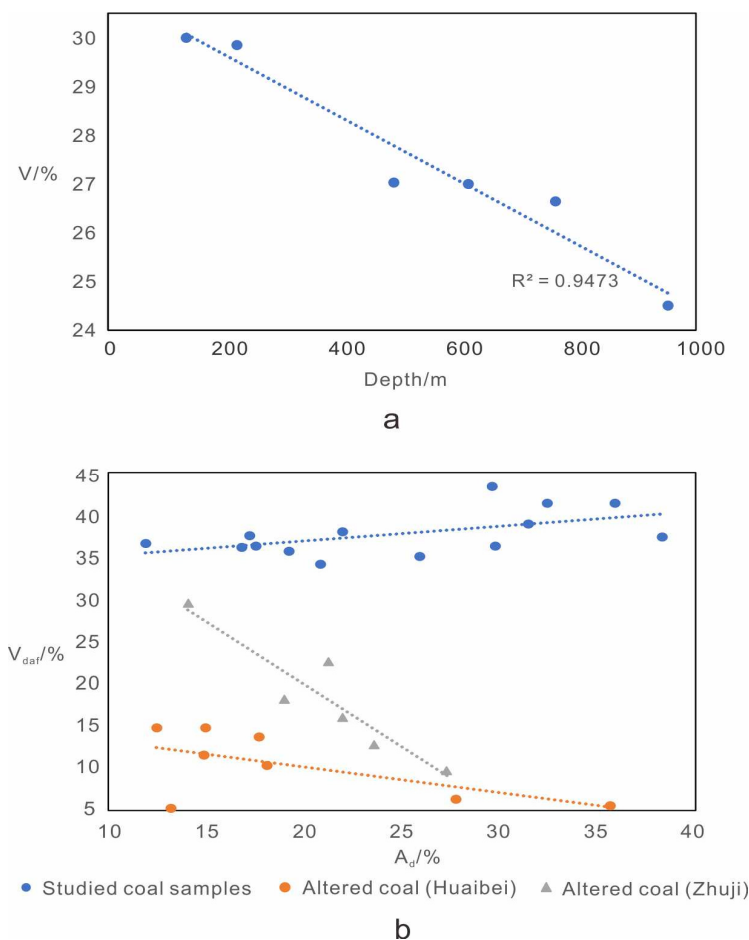
a

b

Figure 9. Volatile matter content variation in Huainan coalfield. (**a**) The correlation between volatile matter and depth of coal seams in the WFG mine [37] and (**b**) the correlation between volatile matter and ash yield (data on altered coal of Huaibei coalfield are quoted from Yao et al. [13]; data on altered coal of the Zhuji mine of the Huainan coalfield from Wu [18]).

6. Conclusions

In this paper, the modes of mineral occurrence, the origin of mineral formation, and the geological evolution of Permian unaltered coals in the Huainan coalfield were investigated and are summarized below:

(1) The studied coal samples were high volatile A bituminous to medium volatile coal, without the influence of igneous intrusion. The ash yield of the coal samples varied between 11.92% and 38.31% (24.80% on average). The total sulfur content and the moisture contents were both low values ranging from 0.13% to 1.51% (average 0.50%) and 0.66% to 1.48% (average 1.00%), respectively;

(2) terrigenous clastic generally occurs as sub-angular to rounded grains and thin layers intimately admixed with the organic matter in particular horizons. The authigenic mineral occurring as cell infillings, as well as nodule siderites and polycrystalline aggregates of pyrite, precipitated during the syngenetic to early diagenetic stages. The cleat infillings, compressed cell infillings, and fracture infillings precipitated in the epigenetic stage. However, pore-fillings can be formed in every stage of peat accumulation to epigenesis, so they cannot be used to determine the formation stage of minerals;

(3) combined with coal quality, mineralogy, and geochemical analysis, the Permian coal in the Huainan coalfield has undergone the following geological evolution: the sedimentary environment of the Shanxi Formation was affected by seawater, and Fe-rich hydrothermal fluids filled into the No. 3 coal seam in the epigenetic stage; the sedimentary environment of the No. 8 coal seam had widespread reduction and acid conditions due to basin subsidence, and sulfate-rich hydrothermal fluids may have

been flowed in peat during deposition stage; in contrast, the peat accumulation environment of the Upper Shihezi Formation was oxidized with a low pH condition, then, alkaline fluid flowed into the No. 13-1 coal seam in the epigenetic stage.

Author Contributions: Q.S. and Q.C. collected coal samples; B.J. and Y.L. performed the experiments; Y.L. analyzed test data, collected evidence, and wrote the manuscript; W.H. acquired funding and revised the initial draft. All authors have read and agreed to the published version of the manuscript.

Conflicts of Interest: The authors declare no conflict of interest.

References

1. Finkelman, R.B.; Dai, S.F.; French, D. The importance of minerals in coal as the hosts of chemical elements: A review. *Int. J. Coal Geol.* **2019**, *212*, 103251. [CrossRef]
2. Dai, S.F.; Finkelman, R.B. Coal geology in China: An overview. *Int. Geol. Rev.* **2018**, *60*, 531–534. [CrossRef]
3. Dai, S.F.; Chou, C.L. Occurrence and origin of minerals in a chamosite-bearing coal of Late Permian age, Zhaotong, Yunnan, China. *Am. Mineral.* **2007**, *92*, 1253–1261. [CrossRef]
4. Wang, X.B.; Dai, S.F.; Ren, D.Y.; Yang, J.Y. Mineralogy and geochemistry of Al-hydroxide/oxyhydroxide mineral-bearing coals of Late Paleozoic age from the Weibei coalfield, southeastern Ordos Basin, North China. *Appl. Geochem.* **2011**, *26*, 1086–1096. [CrossRef]
5. Ward, C.R. Analysis and significance of mineral matter in coal seams. *Int. J. Coal Geol.* **2002**, *50*, 135–168. [CrossRef]
6. Ward, C.R. Analysis, origin and significance of mineral matter in coal: An updated review. *Int. J. Coal Geol.* **2016**, *165*, 1–27. [CrossRef]
7. Dai, S.F.; Ji, D.P.; Ward, C.R.; French, D.; Hower, J.C.; Yan, X.Y.; Wei, Q. Mississippian anthracites in Guangxi Province, southern China: Petrological, mineralogical, and rare earth element evidence for high-temperature solutions. *Int. J. Coal Geol.* **2018**, *197*, 84–114. [CrossRef]
8. Dai, S.F.; Bechtel, A.; Eble, C.F.; Flores, R.M.; French, D.; Graham, I.T.; Hood, M.M.; Hower, J.C.; Korasidis, V.A.; Moore, T.A.; et al. Recognition of peat depositional environments in coal: A review. *Int. J. Coal Geol.* **2020**, *219*, 103383. [CrossRef]
9. Dai, S.F.; Zou, J.H.; Jiang, Y.F.; Ward, C.R.; Wang, X.B.; Li, T.; Xue, W.F.; Liu, S.D.; Tian, H.M.; Sun, X.H.; et al. Mineralogical and geochemical compositions of the Pennsylvanian coal in the Adaohai Mine, Daqingshan Coalfield, Inner Mongolia, China: Modes of occurrence and origin of diaspore, gorceixite, and ammonian illite. *Int. J. Coal Geol.* **2012**, *94*, 250–270. [CrossRef]
10. Liu, X.B. The mineral matter characteristics of some Chinese coals. *J. China Univ. Min. Technol.* **1994**, *23*, 109–114. (In Chinese) [CrossRef]
11. Kong, H.L.; Zeng, R.S.; Zhuang, X.G. Research on the Minerals in Coals. *Acta Petrol. Mineral.* **2001**, *20*, 441–444. (In Chinese) [CrossRef]
12. Spiro, B.F.; Liu, J.J.; Dai, S.F.; Zeng, R.S.; Large, D.; French, D. Marine derived $^{87}Sr/^{86}Sr$ in coal, a new key to geochronology and palaeoenvironment: Elucidation of the India-Eurasia and China-Indochina collisions in Yunnan, China. *Int. J. Coal Geol.* **2019**, *215*. [CrossRef]
13. Yao, Y.B.; Liu, D.M.; Huang, W.H. Influences of igneous intrusions on coal rank, coal quality and adsorption capacity in Hongyang, Handan and Huaibei coalfields, North China. *Int. J. Coal Geol.* **2011**, *88*, 135–146. [CrossRef]
14. Singh, A.K.; Sharma, M.; Singh, M.P. Genesis of natural cokes: Some Indian examples. *Int. J. Coal Geol.* **2008**, *75*, 40–48. [CrossRef]
15. Juster, T.C.; Brown, P.E.; Bailey, S.W. NH_4-bearing illite in very low grade metamorphic rocks associated with coal, northeastern Pennsylvania. *Am. Mineral.* **1987**, *72*, 555–565.

16. Dai, S.F.; Wang, X.B.; Seredin, V.V.; Hower, J.C.; Ward, C.R.; O'Keefe, J.M.K.; Huang, W.H.; Li, T.; Li, X.; Liu, H.D.; et al. Petrology, mineralogy, and geochemistry of the Ge-rich coal from the Wulantuga Ge ore deposit, Inner Mongolia, China: New data and genetic implications. *Int. J. Coal Geol.* **2012**, *90–91*, 72–99. [CrossRef]

17. Yang, M.; Liu, G.J.; Sun, R.Y.; Chou, C.L.; Zheng, L.G. Characterization of intrusive rocks and REE geochemistry of coals from the Zhuji Coal Mine, Huainan Coalfield, Anhui, China. *Int. J. Coal Geol.* **2012**, *94*, 283–295. [CrossRef]

18. Wu, D. *Research on Nano-Structure of Magmatic Contact Metamorphosed Coal (P1) at Huainan Coalfield*; University of Science and Technology of China: Hefei, China, 2014. (In Chinese)

19. Huang, H.; Han, B.W.; Cheng, S.D. Characteristics of REEs in coals from the igneous intrusion area of the Zhuji Coal Mine, Anhui. *Bull. Mineral. Petrol. Geochem.* **2014**, *33*, 493–499. (In Chinese) [CrossRef]

20. Miao, L.; Liu, G.J.; Wu, D.; Wu, B.; Chen, J. Magmatic intrusive age determination and its significance in Western Zhuji No.3 Minefield, Huainan Coalfield. *Coal Geol. China* **2012**, *24*, 1–6. (In Chinese) [CrossRef]

21. Liu, D.M.; Yao, Y.B.; Tang, D.Z.; Tang, S.H.; Che, Y.; Huang, W.H. Coal reservoir characteristics and coalbed methane resource assessment in Huainan and Huaibei coalfields, Southern North China. *Int. J. Coal Geol.* **2009**, *79*, 97–112. [CrossRef]

22. Chen, J.; Liu, G.J.; Li, H.; Wu, B. Mineralogical and geochemical responses of coal to igneous intrusion in the Pansan Coal Mine of the Huainan coalfield, Anhui, China. *Int. J. Coal Geol.* **2014**, *124*, 11–35. [CrossRef]

23. Wei, Q.; Li, X.Q.; Hu, B.L.; Zhang, X.Q.; Zhang, J.Z.; He, Y.K.; Zhang, Y.C.; Zhu, W.W. Reservoir characteristics and coalbed methane resource evaluation of deep-buried coals: A case study of the No.13–1 coal seam from the Panji Deep Area in Huainan Coalfield, Southern North China. *J. Pet. Sci. Eng.* **2019**, *179*, 867–884. [CrossRef]

24. Li, Z.X.; Wei, J.C.; Jin, X.K. High-resolution sequence stratigraphic characterstics in the Permian from Huainan coalfield. *J. Stratigr.* **2000**, *24*, 34–39. (In Chinese) [CrossRef]

25. Hu, B.L.; Gao, D.Y.; Liu, H.H.; Xu, H.J.; Zhang, P.; Sun, F. Relationship between sedimentary facies and source rocks of Permian strata in Huainan coalfield. *Coal Geol. Explor.* **2017**, *45*, 1–6. [CrossRef]

26. Lan, C.Y.; Yang, B.C.; Peng, S.P. Environment for forming major coal seam of Permian coal-bearing series in Huainan coalfield. *J. China Coal Soc.* **1988**, 11–22. (In Chinese) [CrossRef]

27. Sun, R.Y.; Liu, G.J.; Zheng, L.G.; Chou, C.L. Characteristics of coal quality and their relationship with coal-forming environment: A case study from the Zhuji exploration area, Huainan coalfield, Anhui, China. *Energy* **2010**, *35*, 423–435. [CrossRef]

28. Chen, J.; Liu, G.J.; Jiang, M.M.; Chou, C.L.; Li, H.; Wu, B.; Zheng, L.G.; Jiang, D.D. Geochemistry of environmentally sensitive trace elements in Permian coals from the Huainan coalfield, Anhui, China. *Int. J. Coal Geol.* **2011**, *88*, 41–54. [CrossRef]

29. Zhao, Z.G.; Tang, X.Y.; Li, B.F. Geochemistry of rare-earth elements of coal in Huainan mining area. *Acta Sedimentol. Sin.* **2000**, *18*, 453–459. (In Chinese) [CrossRef]

30. Liu, B.X.; Liu, C.P.; Sun, M.C.; Liu, G.J. A study on magmatic intrusion features in Zhuji minefield, Huainan coalfield. *Coal Geol. China* **2010**, *22*, 13–16. (In Chinese) [CrossRef]

31. Zhang, W.Y.; Zhu, W.W.; Dou, X.Z.; Zhao, Z.Y.; Hu, G.Q.; Ding, H.; Yi, X.H. Research progress on coal measure natural gas exploration development in Huaibei and Huainan coalfields. *Coal Sci. Technol.* **2018**, *46*, 245–251. (In Chinese) [CrossRef]

32. ASTM D3173/D3173M-17. *Standard Test Method for Moisture in the Analysis Sample of Coal and Coke*; ASTM International: West Conshohocken, PA, USA, 2017.

33. ASTM D3175-18. *Standard Test Method for Volatile Matter in the Analysis Sample of Coal and Coke*; ASTM International: West Conshohocken, PA, USA, 2018.

34. ASTM D3174-12. *Standard Test Method for Ash in the Analysis Sample of Coal and Coke from Coal*; ASTM International: West Conshohocken, PA, USA, 2018.

35. ASTM D4239-18e1. *Standard Test Method for Sulfur in the Analysis Sample of Coal and Coke Using High-Temperature Tube Furnace Combustion*; ASTM International: West Conshohocken, PA, USA, 2018.

36. Chung, F.H. Quantitative interpretation of X-ray diffraction patterns of mixtures. II. Adiabatic principle of X-ray diffraction analysis of mixtures. *J. Appl. Crystallogr.* **1974**, *7*, 526–531. [CrossRef]

37. Ao, W.H. *The Characteristics of Deep-Seated Coal Seams' Rank/Coal's Structure and Coalification in Huainan Coalfield*; China University of Geosciences (Beijing): Beijing, China, 2013. (In Chinese)

38. Jiang, D.D.; Chen, P.; Tang, X.Y.; Hong, A.N. Characteristic study and geological genesis analysis of pyrite in No.8 coal in Huainan Coalfield. *Coal Geol. China* **2009**, *21*, 22–26. (In Chinese)

39. GB/T 15224.1-2018. *Classification for Quality of Coal, Part 1: Ash Yield*; Chinese National Standard; General Administration of Quality Supervision, Inspection and Quarantine of the People's Republic of China: Beijing, China, 2018. (In Chinese)

40. ASTM D388-15. *Standard Classification of Coals by Rank*; ASTM International: West Conshohocken, PA, USA, 2015.

41. GB/T 15224.2-2010. *Classification for Quality of Coal, Part 2: Sulfur Content*; Chinese National Standard; General Administration of Quality Supervision, Inspection and Quarantine of the People's Republic of China: Beijing, China, 2010. (In Chinese)

42. Ward, C.R.; Christie, P.J. Clays and other minerals in coal seams of the Moura-Baralaba area, Bowen Basin, Australia. *Int. J. Coal Geol.* **1994**, *25*, 287–309. [CrossRef]

43. Mraw, S.C.; De Neufville, J.P.; Freund, H.; Baset, Z.; Gorbaty, M.L.; Wright, F.J. Science of mineral matter in coal. In *Coal Science*; Gorbaty, M., Larsen, J., Wender, I., Eds.; Academic Press: New York, NY, USA, 1983; Volume 2, pp. 1–63. ISBN 0121507025.

44. Dai, S.F.; Zhang, W.G.; Ward, C.R.; Seredin, V.V.; Hower, J.C.; Li, X.; Song, W.J.; Wang, X.B.; Kang, H.; Zheng, L.C.; et al. Mineralogical and geochemical anomalies of late Permian coals from the Fusui Coalfield, Guangxi Province, southern China: Influences of terrigenous materials and hydrothermal fluids. *Int. J. Coal Geol.* **2013**, *105*, 60–84. [CrossRef]

45. Ward, C.R. Minerals in bituminous coals of the Sydney basin (Australia) and the Illinois basin (U.S.A.). *Int. J. Coal Geol.* **1989**, *13*, 455–479. [CrossRef]

46. Li, B.Q.; Zhuang, X.G.; Querol, X.; Moreno, N.; Córdoba, P.; Li, J.; Zhou, J.B.; Ma, X.P.; Liu, S.B.; Shangguan, Y.F. The mode of occurrence and origin of minerals in the Early Permian high-rank coals of the Jimunai depression, Xinjiang Uygur Autonomous Region, NW China. *Int. J. Coal Geol.* **2019**, *205*, 58–74. [CrossRef]

47. Dai, S.F.; Ren, D.Y.; Chou, C.L.; Li, S.S.; Jiang, Y.F. Mineralogy and geochemistry of the No. 6 Coal (Pennsylvanian) in the Junger Coalfield, Ordos Basin, China. *Int. J. Coal Geol.* **2006**, *66*, 253–270. [CrossRef]

48. Dai, S.F.; Hower, J.C.; Ward, C.R.; Guo, W.M.; Song, H.J.; O'Keefe, J.M.K.; Xie, P.P.; Hood, M.M.; Yan, X.Y. Elements and phosphorus minerals in the middle Jurassic inertinite-rich coals of the Muli Coalfield on the Tibetan Plateau. *Int. J. Coal Geol.* **2015**, *144–145*, 23–47. [CrossRef]

49. Love, L.G. Mircro-organisms and the presence of syngenetic pyrite. *Q. J. Geol. Soc. Lond.* **1957**, *113*, 429–440. [CrossRef]

50. Wilkin, R.T.; Barnes, H.L. Formation processes of framboidal pyrite. *Geochim. Cosmochim. Acta* **1997**, *61*, 323–339. [CrossRef]

51. Sweeney, R.E.; Kaplan, I.R. Pyrite framboid formation; Laboratory synthesis and marine sediments. *Econ. Geol.* **1973**, *68*, 618–634. [CrossRef]

52. Kostova, I.; Petrov, O.; Kortenski, J. Mineralogy, geochemistry and pyrite content of Bulgarian subbituminous coals, Pernik Basin. *Geol. Soc. Spec. Publ.* **1996**, *109*, 301–314. [CrossRef]

53. Fu, B.; Liu, G.J.; Liu, Y.; Cheng, S.W.; Qi, C.C.; Sun, R.Y. Coal quality characterization and its relationship with geological process of the Early Permian Huainan coal deposits, southern North China. *J. Geochem. Explor.* **2016**, *166*, 33–44. [CrossRef]

54. Lan, C.Y. The sedimentary environment of the coal-bearing formation of the Permian period in the Huainan coalfield. *J. Anhui Univ. Sci. Technol.* **1984**, *2*, 10–22. (In Chinese)

55. Lan, C.Y. Sedimentary characteristics and environments of Carboniferous Permian coal-bearing rock measures in Huainan-Huaibei coalfields. *J. Anhui Univ. Sci. Technol.* **1989**, *3*, 9–22. (In Chinese)

56. Butler, I.B.; Rickard, D. Framboidal pyrite formation via the oxidation of iron (II) monosulfide by hydrogen sulphide. *Geochim. Cosmochim. Acta* **2000**, *64*, 2665–2672. [CrossRef]

57. Rickard, D. Kinetics of pyrite formation by the H_2S oxidation of iron (II) monosulfide in aqueous solutions between 25 and 125 °C: The rate equation. *Geochim. Cosmochim. Acta* **1997**, *61*, 115–134. [CrossRef]

58. Permana, A.K.; Ward, C.R.; Li, Z.; Gurba, L.W. Distribution and origin of minerals in high-rank coals of the South Walker Creek area, Bowen Basin, Australia. *Int. J. Coal Geol.* **2013**, *116–117*, 185–207. [CrossRef]

59. Dai, S.F.; Tian, L.W.; Chou, C.L.; Zhou, Y.P.; Zhang, M.Q.; Zhao, L.; Wang, J.M.; Yang, Z.; Cao, H.Z.; Ren, D.Y. Mineralogical and compositional characteristics of Late Permian coals from an area of high lung cancer rate in Xuan Wei, Yunnan, China: Occurrence and origin of quartz and chamosite. *Int. J. Coal Geol.* **2008**, *76*, 318–327. [CrossRef]

60. Dai, S.F.; Jiang, Y.F.; Ward, C.R.; Gu, L.D.; Seredin, V.V.; Liu, H.D.; Zhou, D.; Wang, X.B.; Sun, Y.Z.; Zou, J.H.; et al. Mineralogical and geochemical compositions of the coal in the Guanbanwusu Mine, Inner Mongolia, China: Further evidence for the existence of an Al (Ga and REE) ore deposit in the Jungar Coalfield. *Int. J. Coal Geol.* **2012**, *98*, 10–40. [CrossRef]

61. Dong, Y.; Lan, C.Y.; Zeng, Q.P.; Yang, B.C. Lithofacies and paleogeography from Late Carboniferous to early stage of Late Permian in Huainan-Huaibei coalfields. *Coal Geol. Explor.* **1994**, *22*, 9–12. (In Chinese)

62. Diessel, C.; Boyd, R.; Wadsworth, J.; Leckie, D.; Chalmers, G. On balanced and unbalanced accommodation/peat accumulation ratios in the Cretaceous coals from Gates Formation, Western Canada, and their sequence-stratigraphic significance. *Int. J. Coal Geol.* **2000**, *43*, 143–186. [CrossRef]

63. Rimmer, S.M.; Yoksoulian, L.E.; Hower, J.C. Anatomy of an intruded coal, I: Effect of contact metamorphism on whole-coal geochemistry, Springfield (No. 5) (Pennsylvanian) coal, Illinois Basin. *Int. J. Coal Geol.* **2009**, *79*, 74–82. [CrossRef]

64. Querol, X.; Chinchon, S.; Lopez-Soler, A. Iron sulfide precipitation sequence in Albian coals from the Maestrazgo Basin, southeastern Iberian Range, northeastern Spain. *Int. J. Coal Geol.* **1989**, *11*, 171–189. [CrossRef]

65. Chou, C.L. Sulfur in coals: A review of geochemistry and origins. *Int. J. Coal Geol.* **2012**, *100*, 1–13. [CrossRef]

66. Ward, C.R. Mineral matter in low-rank coals and associated strata of the Mae Moh basin, northern Thailand. *Int. J. Coal Geol.* **1991**, *17*, 69–93. [CrossRef]